Published in final edited form as:

Nat Immunol. 2016 April ; 17(4): 414–421. doi:10.1038/ni.3396.

Stromal cells control the epithelial residence of DCs and memory T cells by regulated activation of TGF-β

Javed Mohammed[1], **Lalit K Beura**[2], **Aleh Bobr**[3], **Brian Astry**[1], **Brian Chicoine**[1], **Sakeen W Kashem**[1], **Nathan E Welty**[1], **Botond Z Igyártó**[1], **Sathi Wijeyesinghe**[1], **Emily A Thompson**[2], **Catherine Matte**[4,5], **Laurent Bartholin**[6], **Alesia Kaplan**[7], **Dean Sheppard**[8], **Alina G Bridges**[3], **Warren D Shlomchik**[9,10], **David Masopust**[2], and **Daniel H Kaplan**[1,11,12]

[1]Department of Dermatology, Center for Immunology, University of Minnesota, Minneapolis, Minnesota USA

[2]Department of Microbiology and Immunology, Center for Immunology, University of Minnesota, Minneapolis, Minnesota USA

[3]Department of Laboratory Medicine and Pathology, Mayo Clinic, Rochester, Minnesota, USA

[4]Department of Medicine, Yale University School of Medicine, New Haven, Connecticut, USA

[5]Department of Immunobiology, Yale University School of Medicine, New Haven, Connecticut, USA

[6]Centre de Recherche en Cancérologie de Lyon, INSERM U1052, CNRS UMR5286, Lyon, France

[7]Department of Laboratory Medicine and Pathology, University of Minnesota, Minneapolis, Minnesota, USA

[8]Department of Medicine, University of California, San Francisco, San Francisco, California, USA

[9]Department of Medicine, University of Pittsburgh Cancer Center Institute, Pittsburgh, Pennsylvania, USA

[10]Department of Immunology, University of Pittsburgh Cancer Center Institute, Pittsburgh, Pennsylvania, USA

[11]Department of Dermatology, University of Pittsburgh, Pennsylvania, USA

[12]Department of Immunology, University of Pittsburgh, Pennsylvania, USA

Correspondence should be addressed to: D.H.K. (dankaplan@pitt.edu).

AUTHOR CONTRIBUTIONS

J.M., D.M. and D.H.K. designed and interpreted experiments; J.M. performed most experiments; L.K.B., B.A., B.C., S.W.K., N.E.W., B.Z.I., S.W. and E.A.T. performed experiments and provided technical assistance; C.M. and W.D.S. provided technical and conceptual assistance; L.B. and D.S. provided reagents and technical assistance; A.B., A.K. and A.G.B. collected and analyzed data from control and losartan treated patients; and J.M. and D.H.K. wrote the manuscript and all authors edited it.

COMPETING FINANCIAL INTERESTS

The authors declare no competing financial interests.

Note: Any Supplementary Information and Source Data files are available in the online version of the paper.

Abstract

Cells of the immune system that reside in barrier epithelia provide a first line of defense against pathogens. Langerhans cells (LCs) and $CD8^+$ tissue-resident memory T cells (T_{RM} cells) require active transforming growth factor-β1 (TGF-β) for epidermal residence. Here we found that integrins $\alpha_v\beta_6$ and $\alpha_v\beta_8$ were expressed in non-overlapping patterns by keratinocytes (KCs) and maintained the epidermal residence of LCs and T_{RM} cells by activating latent TGF-β. Similarly, the residence of dendritic cells and T_{RM} cells in the small intestine epithelium also required $\alpha_v\beta_6$. Treatment of the skin with ultraviolet irradiation decreased integrin expression on KCs and reduced the availability of active TGF-β, which resulted in LC migration. Our data demonstrated that regulated activation of TGF-β by stromal cells was able to directly control epithelial residence of cells of the immune system through a novel mechanism of intercellular communication.

The skin is exposed to a wide variety of potential pathogens and commensal microorganisms. Keratinocytes (KCs) that form the stratified squamous epithelium of the epidermis create a physical barrier and also a niche for cells of the immune system that provide an active immunological barrier, notably Langerhans cells (LCs) and $CD8^+$ tissue-resident memory T cells (T_{RM} cells). LCs are a radioresistant, self-renewing subset of dendritic cell (DCs) that reside exclusively in the epidermis[1]. LCs migrate from the epidermis to the skin-draining lymph nodes (LNs), where they present antigen acquired in peripheral tissue to naive and central memory T cells[1]. Migration occurs both homeostatically and in response to microbial or inflammatory cues, including exposure to hapten, ultraviolet (UV) light and skin infection[2,3]. LCs are required for the induction of responses of the T_H17 subset of helper T cells to specific cutaneous infections and also suppress skin immune responses in a variety of contexts[4–9]. T_{RM} cells are a subset of memory T cells that maintain long-term residence in barrier tissues[10]. In the skin, $CD8^+$ T_{RM} cells reside in the epidermis and provide protective memory responses to infection with herpes simplex virus or vaccinia virus[11–13]. They are also thought to mediate autoimmune diseases such as vitiligo and alopecia areata[14,15].

Transforming growth factor-β1 (TGF-β) is a pleotropic cytokine that has been long considered an essential growth factor for LCs[16]. However, TGF-β signaling is also required for LCs to maintain their epidermal residence[17–19]. LCs successfully populate the epidermis in mice with LC-specific genetic ablation of TGF-β receptors (TGF-βRI or TGF-βRII) but spontaneously migrate to skin-draining LNs[17,18]. Notably, LC-specific ablation of TGF-β induces LC migration, which indicates that autocrine TGF-β is required for the epidermal residence of LCs[17]. The homeostasis of T_{RM} cells also depends on TGF-β. $CD8^+$ T_{RM} cells unable to signal through TGF-β receptors fail to express integrin $\alpha_E\beta_7$ (CD103) and do not maintain residence in barrier epithelia[20].

TGF-β is secreted as a biologically inactive complex non-covalently bound to latency-associated peptide (LAP)[21]. Dissociation of LAP from TGF-β can be mediated by the integrins $\alpha_v\beta_6$ and $\alpha_v\beta_8$, which bind to an RGD (Arg-Gly-Asp) sequence in LAP; this allows TGF-β to become biologically active. *In vivo*, the activation of TGF-β by $\alpha_v\beta_6$ and $\alpha_v\beta_8$ in the epidermis is nonredundant[22,23].

Here we found that $\alpha_v\beta_6$ or $\alpha_v\beta_8$ expressed by KCs was required for the maintenance of epidermal LCs. $\alpha_v\beta_6$ and $\alpha_v\beta_8$ were expressed in non-overlapping patterns throughout the epidermis, and ablation or inhibition of $\alpha_v\beta_6$ or $\alpha_v\beta_8$ in KCs reduced the availability of active TGF-β, which resulted in loss of LCs from the epidermal region where that integrin was normally expressed. Similarly, residence of DCs in the epithelium of the small intestine and residence of $CD8^+$ T_{RM} cells in both intestinal epithelium and epidermis required $\alpha_v\beta_6$. In addition, UV irradiation reduced integrin expression by KCs and diminished the amount of activated TGF-β, which resulted in LC migration that was overcome by constitutive TGF-β signaling in LCs. Thus, regulated transactivation of LAP–TGF-β by KCs determined the epithelial residence of both DCs and T_{RM} cells.

RESULTS

Epidermal maintenance of LCs in human skin requires TGF-β

To determine whether the epidermal residence of LCs requires TGF-β signaling in human skin, we compared the number of epidermal LCs in skin samples obtained from untreated (control) patients with that in patients treated with losartan. Losartan is an antagonist to the angiotensin II type I receptor commonly used to treat hypertension but also attenuates TGF-β-mediated pathologies by inhibiting TGF-β signaling through an unknown mechanism[24,25]. The average number of LCs per linear mm of skin was reduced from 21.2 in age- and sex-matched control patients (**Supplementary Table 1**) to 14.3 in losartan-treated patients (Fig. 1a and **Supplementary Fig. 1**). Thus, the maintenance of LCs in human epidermis seemed to require TGF-β.

$\alpha_v\beta_6$ inhibits homeostatic LC migration by activating TGF-β

On the basis of the findings reported above, we hypothesized that homeostatic LC migration would require a loss of TGF-β signaling. To test our hypothesis, we bred huLangerin-$CreER^{T2}$ mice (which have tamoxifen-inducible expression of Cre recombinase from the LC-specific gene encoding human langerin (huLangerin)) with TGF-βRI–CA mice (which express a *lox*P-STOP cassette followed by a mutant, constitutively active (CA), hemagglutinin-tagged form of TGF-βRI that signals independently of ligand) to generate TGF-βRI–CA^{LC} mice (with inducible expression of constitutively active TGF-βRI in LCs)[26]. Treatment of TGF-βRI–CA^{LC} mice with tamoxifen efficiently induced the expression of TGF-βRI–CA in LCs without affecting their viability (**Supplementary Fig. 2a,b**). Notably, ligand-independent TGF-β signaling resulted in a normal number of LCs in the epidermis but significantly fewer LCs in the LNs of TGF-βRI–CA^{LC} mice (Fig. 1b,c), indicative of a failure of homeostatic migration. As a comparison, ablation of TGF-β in LCs produced the opposite phenotype: enhanced migration (Fig. 1b,c).

Since TGF-β is secreted as a latent complex, we next investigated whether its activation was required for the epidermal maintenance of LCs. Consistent with reports of reduced numbers of LCs in integrin β_6–deficient (*Itgb6*−/−) mice22,23, we found spontaneous migration of LCs in *Itgb6*$^{-/-}$ mice (Fig. 1b,c). Similarly, *in vivo* blockade of $\alpha_v\beta_6$ activity in wild-type mice by intradermal injection of a neutralizing antibody resulted in local reduction in the number of LCs but not that of dermal DCs (Fig. 1d,e and **Supplementary Fig. 2c**). Notably,

neutralization of $\alpha_v\beta_6$ in tamoxifen-treated TGF-βRI–CA^{LC} mice did not induce LC migration (Fig. 1d,e). Similarly, tamoxifen treatment largely restored the epidermal LC network in *Itgb6*$^{-/-}$ TGF-βRI–CA^{LC} mice (**Supplementary Fig. 2d,e**). Thus, $\alpha_v\beta_6$-mediated activation of TGF-β was needed to maintain LC residence.

$\alpha_v\beta_6$ on interfollicular KCs controls epidermal LC residence

Since $\alpha_v\beta_6$ is expressed by several epithelial tissues, we next investigated whether it was expressed by KCs in the epidermis. We noticed that KCs in wild-type mice expressed $\alpha_v\beta_6$, as assessed by immunofluorescence of epidermal mounts, but its expression was not uniform throughout the epidermis (Fig. 2a). We defined KCs on the basis of their location and relationship to the hair follicle, as interfollicular (IFE), isthmus (IM) and bulge KCs (**Supplementary Fig. 3a**). Precursors of LCs are recruited into the epidermis first through the IM before they populate the IFE region but are actively excluded from the bulge area[27]. Using surface markers to identify individual KC subsets[27] (**Supplementary Fig. 3b**), we noted that $\alpha_v\beta_6$ expression was evident in the IFE and bulge regions but was absent from the IM (Fig. 2a,b,e). The residual LCs in *Itgb6*$^{-/-}$ mice seemed to 'preferentially' be located in the IM (Fig. 2a). To confirm that observation, we quantified LCs in the IFE region or IM in wild-type and *Itgb6*$^{-/-}$ mice. The number of LCs was significantly lower in the IFE region of *Itgb6*$^{-/-}$ mice than in that of wild-type mice but remained unaffected in the IM of *Itgb6*$^{-/-}$ mice (Fig. 2c). In addition, the few LCs that remained in the epidermis of *Itgb6*$^{-/-}$ mice were located in close proximity to the hair follicle (Fig. 2d).

In the epidermis, *Itgb6* mRNA expression was higher in IFE KCs than in IM KCs, but *Itgb6* mRNA was detectable in LCs (Fig. 2e). To determine whether maintenance of epidermal LCs relied on expression of $\alpha_v\beta_6$ by KCs or LCs, we generated bone marrow (BM) chimeras by reconstituting irradiated wild-type(CD45.2$^+$) recipient mice or *Itgb6*$^{-/-}$ (CD45.2$^+$) recipient mice with congenic wild-type (CD45.1$^+$) BM cells (wild-type→wild-type mice or wild-type→*Itgb6*$^{-/-}$ mice, respectively). A hematopoietic chimerism of >95% was achieved after 6 weeks in blood and LNs (**Supplementary Fig. 4a,b**). As expected, since LC are radio-resistant, they remained of host origin in wild-type mice (Fig. 2f). In contrast, donor-derived LCs were recruited into the epidermis of wild-type→*Itgb6*$^{-/-}$ mice, which resulted in 50% LC chimerism (Fig. 2f and **Supplementary Fig. 4c**). The frequency of host *Itgb6*$^{-/-}$ LCs and donor wild-type LCs in the epidermis were equivalent in wild-type→*Itgb6*$^{-/-}$ mice (Fig. 2f and **Supplementary Fig. 4c**), which indicated that expression of $\alpha_v\beta_6$ by LCs was not required for their retention in the epidermis. Instead, the absence of $\alpha_v\beta_6$ on KCs of wild-type→*Itgb6*$^{-/-}$ mice led to a failure of LC precursors to spread beyond the hair follicle, which resulted in the absence of LCs in the IFE region (Fig. 2g), similar to that seen in *Itgb6*$^{-/-}$ mice. Thus, expression of $\alpha_v\beta_6$ on IFE KCs controlled the epidermal residence of LC.

Non-overlapping expression of $\alpha_v\beta_6$ and $\alpha_v\beta_8$ by KC subsets

In addition to $\alpha_v\beta_6$, $\alpha_v\beta_8$ also activates LAP–TGF-β[21]. $\alpha_v\beta_8$ is expressed by DCs and has a non-redundant role in TGF-β-mediated development of T_H17 cells and regulatory T cells28,29. Expression of $\alpha_v\beta_8$ by epithelial cells, however, has not been reported, to our knowledge. To investigate whether cells in the epidermis expressed $\alpha_v\beta_8$, we compared the

expression of $\alpha_v\beta_8$-encoding mRNA on sorted populations of epidermal cells. Unexpectedly, we detected minimal expression of *Itgb8* (which encodes β_8) in LCs (Fig. 3a). Instead, we found that IM KCs had the highest expression of *Itgb8*, while IFE KCs had much lower expression of *Itgb8* (Fig. 3a), an expression pattern reciprocal to that seen for *Itgb6* (Fig. 2e). This raised the possibility that the presence of LCs in the IM of *Itgb6*$^{-/-}$ mice might have resulted from $\alpha_v\beta_8$-mediated activation of TGF-β.

To test that hypothesis, we bred *Itgb8*^{loxP} mice (which have *lox*P-flanked *Itgb8* alleles) with huLangerin-Cre mice (which express Cre recombinase from the LC-specific gene encoding human langerin) to generate mice with LC-specific ablation of *Itgb8* (*Itgb8*$^{\Delta LC}$), or with K14-Cre mice (which express Cre recombinase from the KC-specific gene encoding keratin 14) to generate mice with KC-specific ablation of *Itgb8* (*Itgb8*$^{\Delta KC}$). The number of LCs in the epidermis and LNs was unaltered in *Itgb8*$^{\Delta LC}$ mice relative to that in wild-type mice (**Supplementary Fig. 5a–c**). In contrast, the number of LCs in skin-draining LNs was elevated and the number of LCs was decreased in IM of the epidermis of *Itgb8*$^{\Delta KC}$ mice, relative to that in wild-type mice (Fig. 3b,c). Notably, the number of LCs was reduced in the IM of the hair follicle but remained unaltered in the IFE region in *Itgb8*$^{\Delta KC}$ mice, relative to that in wild-type mice, as assessed by immunofluorescence imaging of whole tail mounts and transverse sections of back skin (Fig. 3d,e). To exclude the possibility that TGF-β might be activated though mechanisms other than those involving $\alpha_v\beta_6$ or $\alpha_v\beta_8$, we crossed *Itgb8*$^{\Delta KC}$ mice with *Itgb6*$^{-/-}$ mice. The resulting *Itgb8*$^{\Delta KC}$*Itgb6*$^{-/-}$ mice lacked expression of both $\alpha_v\beta_6$ and $\alpha_v\beta_8$ (data not shown) and were devoid of epidermal LCs (Fig. 3f,g), which confirmed the absence of compensatory mechanisms for activation of TGF-β in the epidermis. Finally, we directly investigated the necessity for $\alpha_v\beta_6$ and $\alpha_v\beta_8$ in the KC-mediated activation of latent TGF-β using an *in vitro* assay for activated TGF-β[30]. Primary mouse KCs were co-cultured with mink lung reporter cells that had been transfected with a TGF-β-responsive promoter that drives the expression of luciferase. The ability of KCs to activate latent TGF-β was significantly reduced by antibody blockade of $\alpha_v\beta_6$ in both wild-type cells and *Itgb8*$^{\Delta KC}$ cells, relative to its activation in their counterparts treated with control antibody (Fig. 3h). Similarly, the amount of active TGF-β was lower in cultures of KCs derived from *Itgb8*$^{\Delta KC}$ mice than in cultures of KCs derived from wild-type mice and was further reduced by blockade of $\alpha_v\beta_6$ (Fig. 3h). Together these data supported a model in which inactive LAP–TGF-β secreted by LCs is converted into an active form through the action of either $\alpha_v\beta_6$ or $\alpha_v\beta_8$ expressed by spatially distinct subsets of KCs, which results in the maintenance of LCs in the epidermis.

Intraepithelial DCs expressing integrin $\alpha_E\beta_7$ (CD103) in the small intestine have been reported[31]. Unlike the skin, the epithelium of the small intestine expressed $\alpha_v\beta_6$ but not $\alpha_v\beta_8$ (**Supplementary Fig. 6a**). Blockade of $\alpha_v\beta_6$ via antibody administered weekly for 4 weeks resulted in a reduction in the number of intraepithelial CD103$^+$ DCs, as assessed by immunofluorescence imaging, but did not alter the number of DCs in the lamina propria (**Supplementary Fig. 6b–d**). Thus, residence of DCs in both the skin and intestinal barrier surfaces required epithelial $\alpha_v\beta_6$.

UV irradiation diminishes TGF-β activation by KCs

In addition to their homeostatic migration, LCs migrate in response to exogenous stimuli such as exposure to UV irradiation[2]. We next sought to determine whether reduced release of TGF-β from LAP by KCs expressing $\alpha_v\beta_6$ or $\alpha_v\beta_8$ controlled UV-induced migration. We first exposed the shaved skin of tamoxifen-treated wild-type and TGF-βRI–CA^{LC} mice to UVB at a dose of 100 mJ/cm^2. After 4 d, we observed a nearly complete absence of LCs, as assessed on the basis of expression of major histocompatibility complex (MHC) class II and langerin, in the epidermis of UVB-treated wild-type mice (Fig. 4a,b). The few remaining MHCII$^+$ cells had very low expression of langerin protein (data not shown), which identified them as short-term monocyte-derived cells and not true, long-term LCs[32]. In contrast, many langerin-positive LCs remained in the epidermis of UVB-treated TGF-βRI–CA^{LC} mice (Fig. 4a,b). A similar result was obtained by epicutaneous application of the fluorescent hapten TRITC (**Supplementary Fig. 7**). Notably, LCs in UVB-treated TGF-βRI–CA^{LC} mice had higher expression of the costimulatory molecule CD86 than that of LCs from their counterparts not treated with UVB, indicative of some degree of activation, but failed to increase their expression of CCR7, the chemokine receptor required for the migration of DCs into draining LNs (Fig. 4c). *Ex vivo* KCs from the UVB-irradiated skin of wild-type mice had lower expression of *Itgb6* in IFE KCs and of *Itgb8* in IM KCs than that of their counterparts from wild-type mice not treated with UVB (Fig. 4d). Similarly, UVB irradiation reduced the expression of both *Itgb6* and *Itgb8* in primary cultured wild-type KCs and also reduced the activation of TGF-β by UV irradiation–exposed primary KCs, as measured with luciferase reporter cells (Fig. 4e–g). Thus, in the setting of UV irradiation, KCs reduced their expression of $\alpha_v\beta_6$ and $\alpha_v\beta_8$, which resulted in smaller amounts of active TGF-β. That in turn led to a failure of LCs to maintain epidermal residence that was overcome by constitutive TGF-β signaling.

Epidermal CD8$^+$ T_{RM} cell residence requires $\alpha_v\beta_6$ and $\alpha_v\beta_8$

Studies have demonstrated that local TGF-β is essential for the persistence of T_{RM} cell precursors in the epidermis[20]. CD103 (encoded by *Itgae*) pairs with integrin β_7 to bind the ligand E-cadherin in various epithelial tissues. TGF-β induces CD103 expression on CD8$^+$ T cells in the small intestine, where CD103 is required for the retention of CD8$^+$ T_{RM} cells in the epithelium but not in the underlying lamina propria[33–35]. On the basis of those findings and our own observations, we hypothesized that in addition to maintaining the epidermal residence of LCs, the integrin-mediated activation of TGF-β might also be required for the retention of epidermal T_{RM} cells. To test our hypothesis, we adoptively transferred Thy-1.1$^+$ lymphocytic choriomeningitis virus (LCMV)-specific P14 CD8$^+$ T cells into wild-type, *Itgb6*$^{-/-}$, *Itgb6*$^{-/-}$*Itgb8*$^{\Delta KC}$ or LC-deficient mice, infected the host mice with LCMV (Armstrong strain) and applied the hapten DNFB (an established technique for seeding the epidermis with P14 T cells) topically onto the skin of the host mice[20]. At day 42 after infection, Thy-1.1$^+$ P14 T_{RM} cells were readily detectable in wild-type host mice by immunofluorescence microscopy of epidermal whole mounts (Fig. 5a,b). In contrast, T_{RM} cells were much less frequent in the epidermis of *Itgb6*$^{-/-}$ mice and were completely absent from that of *Itgb6*$^{-/-}$*Itgb8*$^{\Delta KC}$ mice, despite a normal number of these cells in both blood and LNs of *Itgb6*$^{-/-}$ and *Itgb6*$^{-/-}$*Itgb8*$^{\Delta KC}$ mice (Fig. 5a,b and **Supplementary Fig. 8a**).

Host mice that lacked LCs had a normal number of T_{RM} cells (Fig. 5a,b and **Supplementary Fig. 8a**), which indicated that the retention of T_{RM} cells in the epidermis was independent of LCs, consistent with published reports[36].

To exclude the possibility that T cells failed to enter the epidermis of *Itgb6*$^{-/-}$ and *Itgb6*$^{-/-}$*Itgb8*$^{\Delta KC}$ mice, rather than persisting there, we first assessed the number of P14 cells using a strategy similar to that described above, except we analyzed mice at day 7 after infection, which coincided with the effector phase of the T cell response. We observed an equivalent number of P14 cells in the skin, blood and LNs of wild-type, *Itgb6*$^{-/-}$ and *Itgb6*$^{-/-}$*Itgb8*$^{\Delta KC}$ host mice (Fig. 5c,d and **Supplementary Fig. 8b**). Although P14 cells entered the epidermis in similar numbers in all mice, the frequency of such cells that expressed CD103 was significantly lower in *Itgb6*$^{-/-}$ and *Itgb6*$^{-/-}$*Itgb8*$^{\Delta KC}$ mice than in wild-type mice (Fig. 5e), consistent with a requirement for active TGF-β for the expression of CD103 by T_{RM} cells[20,37]. In addition, we treated wild-type recipient mice weekly with neutralizing antibody to $\alpha_v\beta_6$ for 4 weeks starting 56 d after infection, once T_{RM} cell residence had been established. Neutralization of $\alpha_v\beta_6$ in wild-type mice efficiently reduced the number of P14 cells in the epidermis but not in the LNs or blood (Fig. 5f,g and **Supplementary Fig. 8c**), which demonstrated that the epithelial residence of T_{RM} cells required $\alpha_v\beta_6$. Thus, $\alpha_v\beta_6$ and $\alpha_v\beta_8$ were required for the development and maintenance of $CD8^+$ T_{RM} cells in epidermis.

Residence of intestine epithelial $CD8^+$ T_{RM} cells requires $\alpha_v\beta_6$

Since the epithelium of the small intestine expressed $\alpha_v\beta_6$ and blocking $\alpha_v\beta_6$ function *in vivo* led to a reduced number of intraepithelial DCs, we next investigated whether the residence of T_{RM} cells in intestinal epithelium also required $\alpha_v\beta_6$. Using an experimental model similar to that described above to generate LCMV-specific T_{RM} cells, we analyzed wild-type and *Itgb6*$^{-/-}$ mice host mice at both a memory time point (day 42 after infection) and an effector time points (day 7 after infection) to quantify P14 cells in the epithelium and lamina propria of the small intestine. Consistent with our findings obtained for the epidermis, there was a significantly reduced number of T_{RM} cells, with no difference in the entry of P14 cells, during the effector phase in the intestinal epithelium of *Itgb6*$^{-/-}$ mice, compared with that of wild-type mice (Fig. 6a,b,d,e). The number of P14 cells at the memory and effector phases in intestinal lamina propria was similar in *Itgb6*$^{-/-}$ mice and wild-type mice (Fig. 6c,f). Neutralization of $\alpha_v\beta_6$ in wild-type mice after T_{RM} cells had been established (day 56 after infection) efficiently reduced the number of P14 cells in the intestinal epithelium but not in the lamina propria (Fig. 6g–i), which demonstrated that $\alpha_v\beta_6$ was required for the maintenance of T_{RM} cells in the epithelium of the small intestine even after T_{RM} cells had been established.

DISCUSSION

Here we have demonstrated that regulated activation of LC-derived LAP–TGF-β by KCs determined whether LCs migrated from the epidermis. We found that KCs expressed $\alpha_v\beta_6$ and $\alpha_v\beta_8$ in non- overlapping patterns and that deletion or blockade of integrins reduced the availability of active TGF-β, which resulted in loss of LCs from the epidermal region in

which that integrin was normally expressed. The migration of LCs in response to UV irradiation required loss of TGF-β signaling in LCs and was accompanied by reduced expression of integrins by KCs. We also found that expression of $\alpha_v\beta_6$ was required for the persistence of T_{RM} cells in the epidermis and the epithelium of the small intestine. Together these data demonstrate a key role for stromal cells in determining the residence of cells of the immune system within barrier epithelia.

LC migration is thought to result from a combination of LC-intrinsic activation through engagement of pattern-recognition receptors and inflammatory cytokines such as IL-1β and TNF[38]. Our data obtained with TGF-βRI–CA^{LC} mice demonstrated that loss of TGF-β signaling in LCs was required for homeostatic migration and for both UVB-induced migration and hapten-induced migration. Loss of integrin expression by KCs was also sufficient to induce LC migration. Notably, homeostatic and inflammation-induced LC migration is unaffected by the absence of the adaptor MyD88 in LCs[3,39,40]. Thus, we speculate that inflammatory mediators known to drive LC migration might act indirectly through KCs and that reduced activation of TGF-β by KCs is a general mechanism that prompts LC migration. Whether KCs modulate integrin expression in the steady state or in response to inflammatory mediators other than those we have tested, however, remains to be determined.

T_{RM} cell differentiation is induced by environmental factors, of which TGF-β remains the best characterized. As with LCs, T_{RM} cells also depended on the transactivation of TGF-β by KCs for epidermal residence. The number of T_{RM} cells was reduced in *Itgb6*$^{-/-}$ and *Itgb6*$^{-/-}$*Itgb8*$^{\Delta KC}$ mice, and antibody blockade of $\alpha_v\beta_6$ reduced the number of epidermal T_{RM} cells. The recruitment of effector cells into the epidermis was unaffected by the absence of these integrins, but the frequency of cells expressing CD103 was reduced. These results are consistent with a requirement for TGF-β during T_{RM} cell development but also support a model in which tonic exposure to TGF-β, regulated by local TGF-β-activating integrin expression, is constitutively required for their long-term epidermal retention.

Notably, the number of T_{RM} cells was unaffected by the absence of LCs, which indicated that the LCs were not the source of TGF-β that maintained the T_{RM} cells. Dendritic epidermal T cells produced copious amounts of TGF-β (data not shown) but have been reported to remain spatially distinct from T_{RM} cells, so they are unlikely to be critical for the maintenance of T_{RM} cells in the epidermis[36]. KCs are also a major source of TGF-β and probably support epidermal T_{RM} cell residence, although the possibility that TGF-β from T_{RM} cells themselves is involved cannot be excluded. It remains unclear why LCs depend on autocrine TGF-β and do not have access to TGF-β from these other sources.

Epithelial T_{RM} cells in the small intestine require TGF-β for CD103 expression and development[33,34,41]. Unlike integrin expression in the epidermis, $\alpha_v\beta_6$ but not $\alpha_v\beta_8$ was expressed by epithelial cells in the small intestine, consistent with published findings[42]. The absence of T_{RM} cells in *Itgb6*$^{-/-}$ mice and after neutralization of $\alpha_v\beta_6$ demonstrated that, as in the skin, epithelial T_{RM} cells in the intestine also required $\alpha_v\beta_6$ for epithelial retention and probably also for their development. Since $\alpha_v\beta_6$ is widely expressed by many barrier epithelia, T_{RM} cell residence in other tissues might have a similar requirement for this

integrin. $\alpha_v\beta_8$ has been best studied in DCs, in which it provides non-redundant activation of TGF-β and promotes the development of T_H17 cells and regulatory T cells28,29. The unexpected expression of $\alpha_v\beta_8$ by IM KCs raised the possibility that differential regulation of *Itgb6* and *Itgb8* by distinct subsets of KCs might allow regional variation in the leukocyte occupancy of the epidermal niche.

A published report has shown that $CD103^+$ DCs are sparsely distributed in intestinal epithelium during steady state and are recruited from the lamina propria in response to infection[31]. It remains unclear whether steady-state $CD103^+$ DCs represent a true population of intraepithelial DCs or a population that continually migrates between the epithelium and lamina propria. We observed fewer epithelial $CD103^+$ DCs than lamina propria $CD103^+$ DCs after inhibition of $\alpha_v\beta_6$, which suggested that these cells also depended on continuous TGF-β signaling to maintain CD103 expression, similar to T_{RM} cells; thus, these findings potentially extend our findings to epithelial DCs beyond the epidermis.

In summary, we have defined a novel mechanism of retention of DCs and T_{RM} cells in two barrier epithelia through the regulated activation of TGF-β. Compounds that block TGF-β and inhibit $\alpha_v\beta_6$ are in clinical trials as cancer therapeutics and to treat fibrosis during lung, liver and kidney diseases[43]. These compounds might have utility in treating diseases in which T_{RM} cells or LCs are pathogenic. In particular, clearing an established population of T_{RM} cells could be especially effective, since they do not circulate and are unlikely to be replenished without the recruitment of additional $CD8^+$ effector cells. In addition, regulated expression of integrins and activation of TGF-β by stromal cells might participate in numerous other TGF-β-mediated processes, including immunological, carcinogenic, tissue-repair, aging and developmental processes. Whether the regulated transactivation of TGF-β we observed in the epidermis and intestinal epithelium occurs in other barrier and non-barrier tissues as well as other contexts remains to be investigated.

ONLINE METHODS

Mice

huLangerin-Cre, huLangerin-$CreER^{T2}$, TGF-β^{loxP} and TGF-βRI–CA and huLangerin-DTA mice have been previously described[17,26,44]. huLangerin-$CreER^{T2}$ mice were crossed to the TGF-βRI–CA line to generate TGF-βRI–CA^{LC} mice. *Itgb6*$^{-/-}$ and *Itgb8*^{loxP} mice were provided by D. Sheppard (University of California, San Francisco). C57BL/6 (wild-type) and K14-Cre mice were purchased from Jackson Laboratories. K14-Cre and huLangerin-Cre mice were crossed with *Itgb8*^{loxP} mice to obtain *Itgb8*$^{\Delta KC}$ mice and *Itgb8*$^{\Delta LC}$ mice, respectively. We used age-matched female mice that were between 4 and 12 weeks of age in all our experiments. All mice were housed and bred in microisolator cages and were fed irradiated food and acidified water. The University of Minnesota Institutional Care and Use Committee approved all the experimental procedures on mice.

Antibodies

Antibodies 6.3g9 (used for detection of $\alpha_v\beta_6$ by flow cytometry and neutralization of $\alpha_v\beta_6$)45 and ch2A1 (used for detection of $\alpha_v\beta_6$ in mouse epidermis by

immunofluorescence) were provided by S. Violette (Biogen Idec); 6.3g9 was also obtained from American Type Culture Collection. Mouse anti-hemagglutinin (6E2) was purchased from Cell Signaling Technologies. Zenon mouse IgG1 labeling kit (Life Technologies) was used to label 6E2 and 6.3G9 with biotin. Streptavidin–phycoerythrin (PE) and streptavidin–PE–indotricarbocyanine (Cy7) (Life Technologies) were used to detect biotin-labeled antibodies. Anti–collagen IV (AB769) was purchased from EMD Millipore. Fluorochrome-conjugated antibodies to mouse CD3e (145-2c11), CD11b (M1/70), CD11c (N418), CD45.1 (A20), CD45.2 (104), CD80 (16-10A1), CD86 (GL1), CD103 (2E7), Epcam (G8.8), MHCII (M5/114.15.2), Sca-1 (D7) and Thy-1.1 (OX-7) and unconjugated anti–human CD1a (HI149) were purchased from BioLegend. Antibodies to mouse langerin (L31), CCR7 (4B12) and CD49f (eBioGoH3) were purchased from eBioscience. Anti–mouse CD34 (RAM34) was purchased from BD Biosciences. Anti–human langerin (12D6) was purchased from Abcam. Fluorescein-conjugated goat antibody to green fluorescent protein (800-102-215) was purchased from Rockland Immunochemicals. All antibodies and streptavidin reagents were used at a dilution of 1:200, except for anti-CCR7 (1:20), anti-langerin (L31) (1:400) and anti-Thy-1.1 (OX-7) (1:1,000). All antibodies and their dilutions were previously validated in the lab or as recommended by the manufacturer.

Tamoxifen treatment

Tamoxifen (T5648; Sigma-Aldrich) was dissolved in 1/10th volume of 200 proof ethanol following incubation at 37 °C for 15–30 min with occasional vortexing. Corn oil (Sigma-Aldrich) was added for a final concentration of 10 mg/ml and was administered to mice for 5 consecutive days by intraperitoneal injection at 0.05 mg per g of mouse weight.

Histology of human and mice skin

Approval was obtained from Mayo Clinic Institutional Review Board (IRB#13-005614) to search the Mayo Clinic electronic records for patients who were treated with the angiotensin receptor blocker losartan and had undergone excisional biopsy performed for a variety of dermatologic problems. The control group was selected as patients who underwent excisional biopsy and did not receive losartan. Each excisional biopsy had tips of the excision that usually represented unaffected normal tissue, which was confirmed by hematoxylin-and-eosin staining. Slides with pathology and excisions of soles and palms in both groups were excluded. Archived formalin-fixed, paraffin-embedded human skin sections were deparaffinized and subjected to an antigen-retrieval procedure by microwave treatment in citrate buffer (pH 6). After sections cooled to 25 °C, they were blocked with PBS containing 3% BSA and 5% goat serum for 60 min at room temperature. Sections were incubated overnight at 4 °C with anti-CD1a or anti–human langerin (both identified above) and washed, and bound antibodies were detected with horseradish peroxidase–conjugated anti-mouse IgG (115-036-062; Jackson ImmunoResearch). Bound secondary antibodies were detected using a Diaminobenzidine Peroxidase Substrate Kit (Vector) following manufacturer's instructions and were counterstained using Gills hematoxylin (Vector). Epidermal LCs were counted and are presented as linear density number per mm. Mouse skin was embedded in OCT compound and frozen in liquid nitrogen. Transverse mouse skin sections that were 7-μm thick were prepared from frozen blocks using a cryostat and were fixed for 5 min in chilled acetone. Sections were blocked with PBS containing 0.1% tween,

3% BSA and 2% rat normal serum for 60 min before staining overnight with Alexa Fluor 488–conjugated anti–mouse MHC class II and Alexa Fluor 647– conjugated anti-langerin (both identified above) in PBS containing 0.1% tween and 3% BSA. DAPI (4,6-diamidino-2-phenylindole) was used for nuclear counterstaining. Images were captured using Leica DM5500 epifluorescent microscope with digital system and LAS AF software (version 1.5.1).

Immunofluorescence of epidermis

Epidermal whole mounts for immunofluorescence were prepared as previously described[8]. Epidermal sheets were prepared from ear, back and tail skin by affixing of the epidermis side to slides with double-sided adhesive (3M). Slides were incubated in 10 mM EDTA in PBS for 2 h at 37 °C, followed by physical removal of the dermis. Epidermal mounts were fixed in chilled acetone for 5 min. They were subsequently stained and images captured similar to transverse skin sections mentioned above. LCs and T_{RM} cells in epidermis were counted either by ImageJ software or manually in a blinded fashion.

Freezing, immunofluorescence and microscopy of small intestine

Harvested mouse small intestines were frozen as described[46]. Specimens were embedded in the tissue-freezing medium OCT and were snap-frozen in an isopentane liquid bath. Frozen blocks were cut to prepare 7-μm-thick sections using a Leica cryostat. Immunofluorescence microscopy was performed using a Leica DM5500 B microscope six-color fluorescent system with motorized z-focus stage for fully automated image stitching. Separate images taken with a 20× objective were collected for each channel and overlaid to obtain a multicolor image. Image processing and enumeration was done using ImageJ64 and Adobe Photoshop (version 6) as described[47]. Enumeration of $MHCII^+$ DCs and P14 $CD8^+$ T cells was done manually in Adobe Photoshop, and ImageJ64 software was used to enumerate nuclei in each image. All software-based counts were periodically manually validated.

Flow cytometry

Epidermal and LN single-cell suspensions were prepared for flow cytometry as previously described[8]. Single-cell suspensions of epidermal cells were obtained from trunk or ear skin and were incubated for 2 h at 37 °C in 0.3% trypsin (Sigma-Aldrich) in 150 mM NaCl, 0.5 mM KCl and 0.5 mM glucose. The epidermis was physically separated from the dermis and disrupted by mincing and vigorous pipetting. The resulting cells were filtered through a 40-μm filter. LNs (axillary, brachial and inguinal) were incubated in 400 U/ml collagenase D (Roche Applied Science) for 30 min before filtration through a 40-μm filter. Single-cell suspensions were pretreated for 10 min with blocking antibody to CD16/CD32 (2.4G2; American Type Culture Collection) and were stained with antibodies to extracellular markers (all identified above) at 4 °C. For staining of CCR7, epidermal single cells were incubated at room temperature for 60 min. The fixable viability dye eFluor 780 (eBioscience) was used for live-dead discrimination. Intracellular staining of langerin, $\alpha_v\beta_6$ and green fluorescent protein was performed with a BD Bioscience Cytofix/Cytoperm kit (BD Biosciences) in accordance with the manufacturer's instructions. Anti-$\alpha_v\beta_6$ and anti-hemagglutinin (identified above) were labeled with biotin using the zenon mouse IgG1 labeling kit followed by incubation with streptavidin-PE or streptavidin-PE-Cy7. Samples

were analyzed on LSRII flow cytometers (BD Biosciences). Data were analyzed with FlowJo software (TreeStar, Ashland, OR).

Generation of chimeric mice

6-week-old *Itgb6*$^{-/-}$ and wild type C57BL/6 CD45.2 mice were lethally irradiated using a X-ray irradiator and received two split doses of 500 cGy each. The following day, BM cells were prepared following erythrocyte lysis using ACK lysis buffer (Biowhittaker) from congenically marked C57BL/6 CD45.1 mice, and 5×10^6 BM cells injected intravenously into irradiated mice. Mice were rested for at least 6 weeks before experiments. The efficiency of chimerism was determined by flow cytometry of congenic markers on peripheral blood mononuclear cells, spleen, LN and epidermis (antibodies identified above).

Neutralization of $\alpha_v\beta_6$ activity *in vivo*

TGF-βRI–CA^{LC} and wild-type control mice were treated with tamoxifen as described above and injected intradermally with 20 μl in ear of 1 mg/ml anti-$\alpha_v\beta_6$ (6.3g9) or isotype-matched control antibody (ADWA-21; provided by D. Sheppard) under ketamine and xylazine sedation (100 mg and 10 mg/kg body weight, respectively) on days 2 and 5 of tamoxifen treatment. Epidermis was analyzed 3 d following the second antibody injection. In some experiments, 3g9 was administered intra-peritoneally at a dose of 10 mg/kg weekly for up to 4 weeks.

UVB irradiation of mice

TGF-βRI–CA^{LC} and wild-type control mice were treated with tamoxifen as described above. Mice were sedated and backs shaved using hair clippers on third day of tamoxifen treatment. Shaved backs were exposed to 100 mJ/cm^2 UV-B radiation using two TL 20W/12RS bulbs (Philips). Tissues were harvested 4 d after UV irradiation.

Epidermal cell sorting

Epidermal single cells were prepared as described above. Dead cells were gated out using fixable viability dye efluor 780 (eBioscience). Different epidermal cell types were identified and sorted on FACSAria cell sorter using the following markers (antibodies identified above): dendritic epidermal T cells, CD45$^+$CD3e$^+$; LCs, CD45$^+$MHCII$^+$; IFE KCs, CD45$^-$Sca1$^+$CD49f$^+$CD34$^-$; IM KCs, CD45$^-$Sca1$^-$CD34$^-$Epcam$^+$; bulge KCs, CD45$^-$Sca1$^-$CD34$^+$. Purity of the sorted cells was determined by post-sort analysis and consistently exceeded 95%.

Cell culture

Mink lung epithelial reporter cells stably transfected with a plasmid containing luciferase-encoding cDNA downstream of a TGF-β-sensitive portion of the plasminogen activator inhibitor 1 promoter (tMLEC) were cultured as previously described[30]. Primary KCs from newborn mice were prepared and cultured according to established method[48]. Skin was floated overnight with dermis side down at 4 °C in 0.25% trypsin (25 050-Cl; Corning Cellgro). The following day, epidermis was separated from dermis, and single cells were prepared by mincing and vigorous pipetting. After filtration using 100-μm filters, epidermal

cells were plated overnight in Eagle's MEM (06-174G, Lonza) supplemented with 1.4 mmol/L $CaCl_2$ and 8% chelexed FCS. After 16–20 h of culture, the dishes were washed twice with PBS and Eagle's MEM with 8% chelexed serum and 0.05 mmol/L $CaCl_2$ (KC medium) was added that was replaced every 2 d. Primary KCs were cultured to at least 90% confluence before being treated with 50 mJ/cm^2 UVB radiation.

RNA isolation and quantitative PCR

Total RNA from flow cytometry–sorted epidermal cells and primary KC cultures was extracted with the RNeasy Mini extraction kit (Qiagen) following the manufacturer's instructions and was quantified using Nanodrop (NanoDrop). cDNA was generated using a High Capacity cDNA Reverse Transcription Kit (Applied Biosystems) and was subjected to quantitative PCR using TaqMan Gene Expression Master Mix and TaqMan Gene Expression Assays for *Hprt*, *Itgb6*, *Itgb8*, *Itgav* and *Fermt1* (Kindlin-1). ABI Prism 7900HT (Applied Biosystems) was used to complete the quantitative PCR. All protocols while using the kits were completed according the manufacturer's instructions. All cycling threshold (Ct) values were normalized to *Hprt* expression.

Latent TGF-β-activation assay

Latent TGF-β activation by KCs was determined by coculture with thymic mink lung epithelial cells (tMLECs) as described[49]. tMLEC were resuspended in DMEM containing 10% FCS and were plated at 1.6×10^4 cells/well of a 96-well cell culture treated plate for 3 h at 37 °C and 5% CO_2. Control primary KCs and UVB-exposed KCs were harvested from the culture dish by gentle trypsinization using 0.25% trypsin and 2.21 mM EDTA (25 053-Cl; Corning Cellgro). KCs were resuspended at 2×10^5 cells/ml in KC medium with 1% chelexed serum, and 100 μl was added to tMLEC cultures after replacement of the medium. Separate groups of KCs were pre-incubated with 10 μg/ml anti-$\alpha_v\beta_6$ (6.3g9) for 60–90 min before addition to tMLEC cultures. The cells were cultured for 16–20 h, following which the reporter cells were lysed and assayed for luciferase activity using Bright Glo Luciferase Assay System (Promega).

Generation of P14 immune chimeras and treatments

5×10^4 naive Thy-1.1^+ P14 T cells ($CD8^+$ T cells with transgenic expression of a T cell antigen receptor specific to the LCMV epitope of glycoprotein amino acids 33–41) were transferred intravenously into wild-type, *Itgb6*$^{-/-}$ or *Itgb6*$^{-/-}$*Itgb8*$^{\Delta KC}$ mice on day -1, followed by infection with LCMV Armstrong strain (2×10^5 plaque-forming units per mouse) on day 0. The contact-sensitizing agent 2,4-dinitrofluorobenzene (DNFB) was applied on skin at day 3 to pull effector P14 cells to the site of sensitization. For this, a ~1-cm^2 area on mice skin was shaved, and 20 μL of 0.2% DNFB in acetone–olive oil (4:1) was applied. Tissues were harvested either on day 7 or day 42 for analysis. Separate cohorts of wild-type mice were injected intraperitoneally weekly for 4 weeks with 10 mg/kg isotype-matched control antibody (ADWA-21; provided by D. Sheppard) or anti-$\alpha_v\beta_6$ (6.3g9) starting at day 56 after infection. Separate cohorts of wild-type mice were also injected intraperitoneally with isotype-matched control antibody (ADWA-21; provided by D. Sheppard) or anti-$\alpha_v\beta_6$ (6.3g9) on days 2 and 5 after infection and were analyzed 3 d later (day 8 after infection).

Statistical analysis

All the statistical analysis on the data was done using GraphPad Prism software version 6.0. Statistical significance of differences between two groups with normally distributed data was determined using Student's unpaired two-tailed *t*-test. For data that did not distribute normally between two groups, a two-tailed Mann-Whitney test was done. For groups of more than two, a one-way analysis of variance was used along with Tukey's post-analysis tests. Sample sizes were chosen based on prior experiences with experimental mouse models. Mice of a particular genotype were randomly assigned to various treatment groups within a study. Blinding was used to count positive cells in immunofluorescent images in Figures 5 and 6.

Acknowledgments

We thank D. Sheppard (University of California, San Francisco) for *Itgb6*$^{-/-}$ and *Itgb8*^{loxP} mice and the isotype-matched control antibody ADWA-21; A. Glick, N. Blazanin and A. Ravindran for technical assistance with mouse KC culture; S. Violette (Biogen Idec) for antibody clones 6.3g9 and ch2A1 (both specific for $\alpha_V\beta_6$); J. Mitchell for technical assistance with confocal and epifluorescence microscopy; T. Martin, J. Motl and P. Champoux for technical assistance with flow cytometry and cell sorting; D. Rifkin and M. Vassallo for providing detailed protocols of an *in vitro* latent TGF-β-activation assay; the Research Animal Resources staff at the University of Minnesota for animal care; the Mayo Clinic division of Biostatistics and Bioinformatics for assistance in searching control and losartan-treated skin samples; and M. Jenkins for critical reading of the manuscript. Supported by the US National Institutes of Health (AR060744 to D.H.K., AI084913 to D.M.), the Dermatology Foundation (J.M.) and the American Skin Association (J.M.).

References

1. Merad M, Ginhoux F, Collin M. Origin, homeostasis and function of Langerhans cells and other langerin-expressing dendritic cells. Nat Rev Immunol. 2008; 8:935–947. [PubMed: 19029989]
2. Merad M, et al. Langerhans cells renew in the skin throughout life under steady-state conditions. Nat Immunol. 2002; 3:1135–1141. [PubMed: 12415265]
3. Haley K, et al. Langerhans cells require MyD88-dependent signals for *Candida albicans* response but not for contact hypersensitivity or migration. J Immunol. 2012; 188:4334–4339. [PubMed: 22442445]
4. Igyártó BZ, et al. Skin-resident murine dendritic cell subsets promote distinct and opposing antigen-specific T helper cell responses. Immunity. 2011; 35:260–272. [PubMed: 21782478]
5. Kobayashi T, et al. Dysbiosis and staphylococcus aureus colonization drives inflammation in atopic dermatitis. Immunity. 2015; 42:756–766. [PubMed: 25902485]
6. King JK, et al. Langerhans cells maintain local tissue tolerance in a model of systemic autoimmune disease. J Immunol. 2015; 195:464–476. [PubMed: 26071559]
7. Kautz-Neu K, et al. Langerhans cells are negative regulators of the anti-Leishmania response. J Exp Med. 2011; 208:885–891. [PubMed: 21536741]
8. Kaplan DH, Jenison MC, Saeland S, Shlomchik WD, Shlomchik MJ. Epidermal langerhans cell-deficient mice develop enhanced contact hypersensitivity. Immunity. 2005; 23:611–620. [PubMed: 16356859]
9. Obhrai JS, et al. Langerhans cells are not required for efficient skin graft rejection. J Invest Dermatol. 2008; 128:1950–1955. [PubMed: 18337832]
10. Schenkel JM, Masopust D. Tissue-resident memory T cells. Immunity. 2014; 41:886–897. [PubMed: 25526304]
11. Gebhardt T, et al. Memory T cells in nonlymphoid tissue that provide enhanced local immunity during infection with herpes simplex virus. Nat Immunol. 2009; 10:524–530. [PubMed: 19305395]
12. Jiang X, et al. Skin infection generates non-migratory memory CD8$^+$ T_{RM} cells providing global skin immunity. Nature. 2012; 483:227–231. [PubMed: 22388819]

13. Ariotti S, et al. T cell memory. Skin-resident memory $CD8^+$ T cells trigger a state of tissue-wide pathogen alert. Science. 2014; 346:101–105. [PubMed: 25278612]
14. Rashighi M, et al. CXCL10 is critical for the progression and maintenance of depigmentation in a mouse model of vitiligo. Sci Transl Med. 2014; 6:223ra23.
15. Bertolini M, Uchida Y, Paus R. Toward the clonotype analysis of alopecia areata-specific, intralesional human $CD8^+$ T lymphocytes. J Investig Dermatol Symp Proc. 2015; 17:9–12.
16. Li MO, Flavell RA. TGF-β: a master of all T cell trades. Cell. 2008; 134:392–404. [PubMed: 18692464]
17. Bobr A, et al. Autocrine/paracrine TGF-β1 inhibits Langerhans cell migration. Proc Natl Acad Sci USA. 2012; 109:10492–10497. [PubMed: 22689996]
18. Kel JM, Girard-Madoux MJH, Reizis B, Clausen BE. TGF-β is required to maintain the pool of immature Langerhans cells in the epidermis. J Immunol. 2010; 185:3248–3255. [PubMed: 20713882]
19. Yasmin N, et al. Identification of bone morphogenetic protein 7 (BMP7) as an instructive factor for human epidermal Langerhans cell differentiation. J Exp Med. 2013; 210:2597–2610. [PubMed: 24190429]
20. Mackay LK, et al. The developmental pathway for $CD103^+CD8^+$ tissue-resident memory T cells of skin. Nat Immunol. 2013; 14:1294–1301. [PubMed: 24162776]
21. Travis MA, Sheppard D. TGF-β activation and function in immunity. Annu Rev Immunol. 2014; 32:51–82. [PubMed: 24313777]
22. Yang Z, et al. Absence of integrin-mediated TGFβ1 activation in vivo recapitulates the phenotype of TGFβ1-null mice. J Cell Biol. 2007; 176:787–793. [PubMed: 17353357]
23. Aluwihare P, et al. Mice that lack activity of αvβ6- and αvβ8-integrins reproduce the abnormalities of Tgfb1- and Tgfb3-null mice. J Cell Sci. 2009; 122:227–232. [PubMed: 19118215]
24. Cohn RD, et al. Angiotensin II type 1 receptor blockade attenuates TGF-β-induced failure of muscle regeneration in multiple myopathic states. Nat Med. 2007; 13:204–210. [PubMed: 17237794]
25. Lanz TV, et al. Angiotensin II sustains brain inflammation in mice via TGF-β. J Clin Invest. 2010; 120:2782–2794. [PubMed: 20628203]
26. Bartholin L, et al. Generation of mice with conditionally activated transforming growth factor β signaling through the TGFβ1/ALK5 receptor. Genesis. 2008; 46:724–731. [PubMed: 18821589]
27. Nagao K, et al. Stress-induced production of chemokines by hair follicles regulates the trafficking of dendritic cells in skin. Nat Immunol. 2012; 13:744–752. [PubMed: 22729248]
28. Melton AC, et al. Expression of αvβ8 integrin on dendritic cells regulates Th17 cell development and experimental autoimmune encephalomyelitis in mice. J Clin Invest. 2010; 120:4436–4444. [PubMed: 21099117]
29. Travis MA, et al. Loss of integrin $\alpha_v\beta_8$ on dendritic cells causes autoimmunity and colitis in mice. Nature. 2007; 449:361–365. [PubMed: 17694047]
30. Abe M, et al. An assay for transforming growth factor-β using cells transfected with a plasminogen activator inhibitor-1 promoter-luciferase construct. Anal Biochem. 1994; 216:276–284. [PubMed: 8179182]
31. Farache J, et al. Luminal bacteria recruit $CD103^+$ dendritic cells into the intestinal epithelium to sample bacterial antigens for presentation. Immunity. 2013; 38:581–595. [PubMed: 23395676]
32. Seré K, et al. Two distinct types of Langerhans cells populate the skin during steady state and inflammation. Immunity. 2012; 37:905–916. [PubMed: 23159228]
33. El-Asady R, et al. TGF-β-dependent CD103 expression by $CD8^+$ T cells promotes selective destruction of the host intestinal epithelium during graft-versus-host disease. J Exp Med. 2005; 201:1647–1657. [PubMed: 15897278]
34. Casey KA, et al. Antigen-independent differentiation and maintenance of effector-like resident memory T cells in tissues. J Immunol. 2012; 188:4866–4875. [PubMed: 22504644]
35. Masopust D, et al. Dynamic T cell migration program provides resident memory within intestinal epithelium. J Exp Med. 2010; 207:553–564. [PubMed: 20156972]

36. Zaid A, et al. Persistence of skin-resident memory T cells within an epidermal niche. Proc Natl Acad Sci USA. 2014; 111:5307–5312. [PubMed: 24706879]
37. Park CO, Kupper TS. The emerging role of resident memory T cells in protective immunity and inflammatory disease. Nat Med. 2015; 21:688–697. [PubMed: 26121195]
38. Merad M, Sathe P, Helft J, Miller J, Mortha A. The dendritic cell lineage: ontogeny and function of dendritic cells and their subsets in the steady state and the inflamed setting. Annu Rev Immunol. 2013; 31:563–604. [PubMed: 23516985]
39. Harberts E, Zhou H, Fishelevich R, Liu J, Gaspari AA. Ultraviolet radiation signaling through TLR4/MyD88 constrains DNA repair and plays a role in cutaneous immunosuppression. J Immunol. 2015; 194:3127–3135. [PubMed: 25716994]
40. Wilson NS, et al. Normal proportion and expression of maturation markers in migratory dendritic cells in the absence of germs or Toll-like receptor signaling. Immunol Cell Biol. 2008; 86:200–205. [PubMed: 18026177]
41. Zhang N, Bevan MJ. Transforming growth factor-β signaling controls the formation and maintenance of gut-resident memory T cells by regulating migration and retention. Immunity. 2013; 39:687–696. [PubMed: 24076049]
42. Knight PA, et al. Enteric expression of the integrin αvβ6 is essential for nematode-induced mucosal mast cell hyperplasia and expression of the granule chymase, mouse mast cell protease-1. Am J Pathol. 2002; 161:771–779. [PubMed: 12213704]
43. Akhurst RJ, Hata A. Targeting the TGFβ signalling pathway in disease. Nat Rev Drug Discov. 2012; 11:790–811. [PubMed: 23000686]
44. Kaplan DH, et al. Autocrine/paracrine TGFβ1 is required for the development of epidermal Langerhans cells. J Exp Med. 2007; 204:2545–2552. [PubMed: 17938236]
45. Weinreb PH, et al. Function-blocking integrin αvβ6 monoclonal antibodies: distinct ligand-mimetic and nonligand-mimetic classes. J Biol Chem. 2004; 279:17875–17887. [PubMed: 14960589]
46. Beura LK, et al. Lymphocytic choriomeningitis virus persistence promotes effector-like memory differentiation and enhances mucosal T cell distribution. J Leukoc Biol. 2015; 97:217–225. [PubMed: 25395301]
47. Steinert EM, et al. Quantifying memory CD8 T cells reveals regionalization of immunosurveillance. Cell. 2015; 161:737–749. [PubMed: 25957682]
48. Dlugosz AA, Glick AB, Tennenbaum T, Weinberg WC, Yuspa SH. Isolation and utilization of epidermal keratinocytes for oncogene research. Methods Enzymol. 1995; 254:3–20. [PubMed: 8531694]
49. Annes JP, Chen Y, Munger JS, Rifkin DB. Integrin αvβ6-mediated activation of latent TGF-β requires the latent TGF-β binding protein-1. J Cell Biol. 2004; 165:723–734. [PubMed: 15184403]

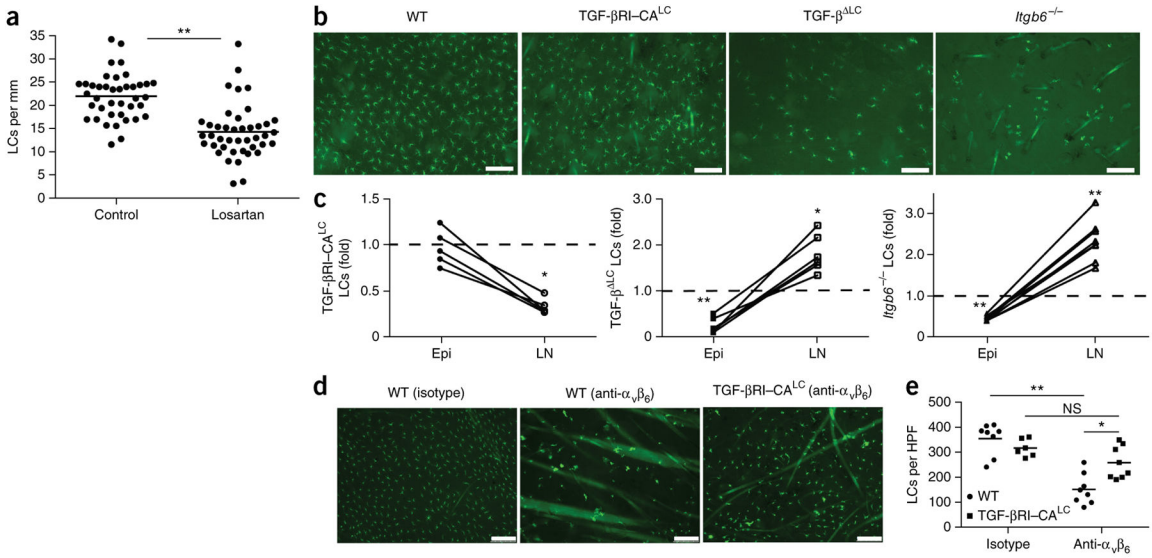

Figure 1.

Activation of latent TGF-β by $\alpha_v\beta_6$ inhibits homeostatic LC migration. (**a**) Quantification of LCs in archival skin specimens from untreated (control) and losartan-treated patients, detected by immunohistochemistry with antibody to CD1a (anti-CD1a) or anti-langerin. Each symbol represents an individual patient; horizontal lines indicate the average. (**b**) Microscopy of whole mounts of back epidermis from cohorts (n = 10 mice in each) of wild-type mice (WT), TGF-βRI–CA^{LC} mice (with inducible expression of constitutively active TGF-βRI in LCs) and TGF-β^{LC} mice (with inducible ablation of TGF-β in LCs) 9 d after the start of tamoxifen treatment, as well as epidermis from adult *Itgb6*$^{-/-}$ mice, all stained for MHC class II (green). (**c**) Ratio of the number of LCs in the epidermis (Epi) (obtained by counting of the MHCII$^+$ cells in **b**) or skin draining LNs (LN) (obtained by flow cytometry) of *Itgb6*$^{-/-}$, TGF-βRI–CA^{LC} and TGF-β^{LC} mice to that in their wild-type counterparts. Each symbol represents an individual mouse (with results from the same mouse joined by a solid line); dashed horizontal lines indicate a ratio of 1.0. (**d**) Microscopy of whole mounts of ear epidermis from tamoxifen-treated wild-type and TGF-βRI–CA^{LC} mice given intradermal injection of anti-$\alpha_v\beta_6$ or isotype-matched control antibody (Isotype) (n = 4 mice per genotype per group), stained for MHC class II (green). (**e**) Quantification of LCs per high-power field (HPF) in the mice in **d**. Each symbol represents LCs per HPF; small horizontal lines indicate the average. Scale bars (**b**,**d**), 100 μm. NS, not significant ($P > 0.05$); *$P < 0.01$ and **$P < 0.0001$ (two-tailed unpaired Student's t test (**a**,**c**) or Tukey's multiple comparisons test (**e**)). Data are representative of experiments with n = 42 total donors (**a**) or are representative of (**b**,**d**) or pooled from (**c**,**e**) three independent experiments.

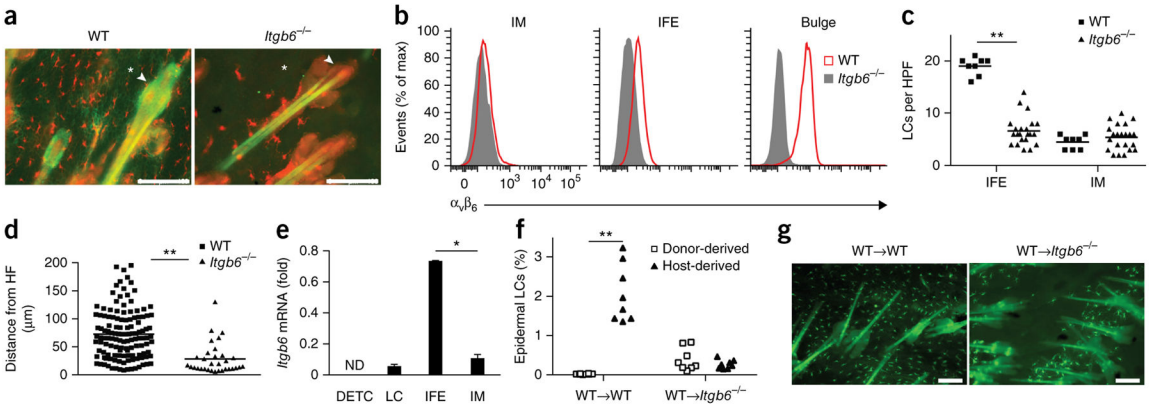

Figure 2.

Epidermal residence of LCs requires expression of $\alpha_v\beta_6$ by IFE epidermal KCs. (**a**) Microscopy of whole mounts of back epidermis from wild-type and *Itgb6*$^{-/-}$ mice, stained for MHC class II (red) and $\alpha_v\beta_6$ (green); arrowheads indicate bulge region of telogen hair; asterisks indicate IFE region. (**b**) Flow cytometric analysis of the expression of $\alpha_v\beta_6$ by IM, IFE and bulge KCs (identified as in **Supplementary Fig. 3b**) from the back skin of wild-type and *Itgb6*$^{-/-}$ mice (key). (**c**) Quantification of LCs in transverse sections of back skin from wild-type and *Itgb6*$^{-/-}$ mice, identified by colocalization of langerin and MHC class II within the IFE region or IM. (**d**) Distance of IFE LCs from the hair follicle (HF) in sections as in **c**. (**e**) Quantitative RT-PCR analysis of *Itgb6* mRNA in sorted epidermal populations of dendritic epidermal T cells (DETC), LCs, and IFE and IM KCs in wild-type mice; results are presented relative to those of the control gene *Hprt*. (**f**) Frequency of host- and donor-derived epidermal LCs in lethally irradiated wild-type→wild-type (WT→WT) or wild-type→*Itgb6*$^{-/-}$ (WT→*Itgb6*$^{-/-}$) (CD45.2$^+$) chimeras 6–8 weeks after transfer of BM from wild-type (CD45.1$^+$) donors, analyzed by flow cytometry. (**g**) Microscopy of whole mounts of back epidermis from chimeras as in **f**, stained for MHC class II (green); autofluorescence shows hair shafts. Scale bars (**a**,**g**), 100 μm. ND, not detected. Each symbol (**c**,**d**,**f**) represents LCs per HPF (**c**), distance from HF (**d**) or an individual mouse (**f**); small horizontal lines indicate the mean. *$P < 0.01$ and **$P < 0.0001$ (two-tailed unpaired Student's *t* test). Data are representative of three independent experiments with eight mice per genotype (**a**,**b**,**g**) or six independent experiments (**e**; mean + s.e.m.) or are pooled from two independent experiments with two mice per group (**c**,**d**) or three independent experiments (**f**).

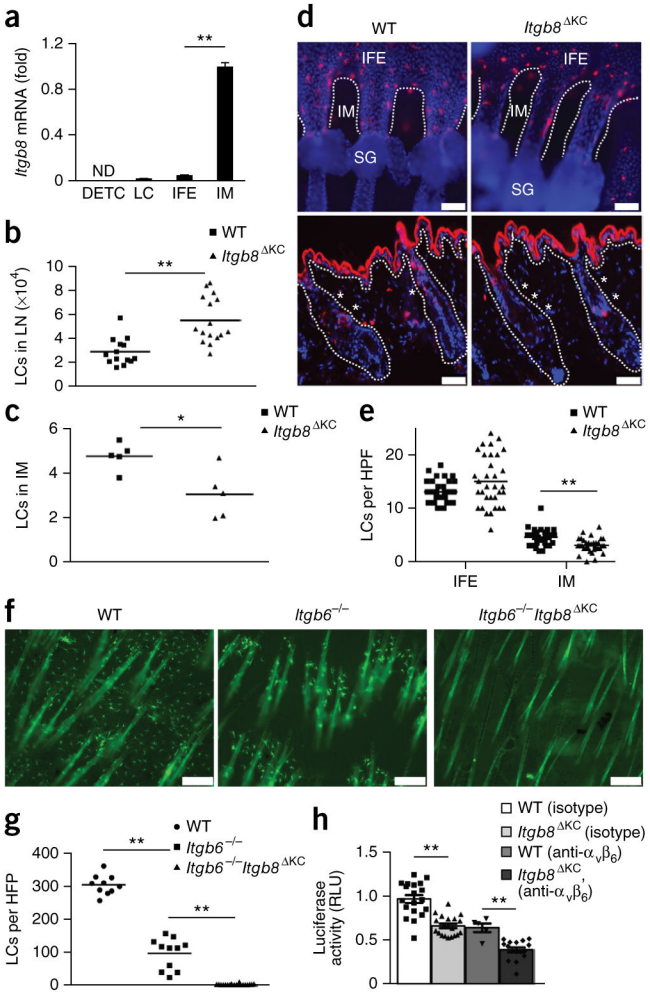

Figure 3.

LC residence is controlled by spatially distinct expression of $\alpha_v\beta_6$ and $\alpha_v\beta_6$ on KC subsets through activation of latent-TGF-β. (**a**) Quantitative RT-PCR analysis of *Itgb8* mRNA in sorted epidermal populations from wild-type mice (as in Fig. 2e). (**b**) Quantification of LCs in skin-draining LNs of wild-type and *Itgb8*$^{\Delta KC}$ mice. (**c**) Quantification of LCs (per HPF) in IM of wild-type and *Itgb8*$^{\Delta KC}$ mice (as in Fig. 2c). (**d**) Microscopy of whole mounts of tail epidermis (top) and transverse sections of back skin (bottom) from wild-type and *Itgb8*$^{\Delta KC}$ mice, stained for langerin (red) and with the DNA-binding dye DAPI (blue); dashed lines, dermal-epidermal junction; SG, sebaceous gland; asterisks (bottom), IM. (**e**) Quantification of LCs in the IFE region and IM of the stained transverse skin sections in **d**. (**f**) Microscopy of whole mounts of back epidermis from wild-type, *Itgb6*$^{-/-}$ and *Itgb6*$^{-/-}$*Itgb8*$^{\Delta KC}$ mice, stained for MHC class II (green); autofluorescence shows hair shafts. (**g**) Quantification of LCs in **f**. (**h**) Luciferase activity in mink lung TGF-β reporter cells cultured together with wild-type or *Itgb8*$^{\Delta KC}$ primary KCs pre-incubated with anti-$\alpha_v\beta_6$ or isotype-matched control antibody; results are presented as relative light units (RLU), normalized to those of wild-type control cells. Each symbol (**b**,**c**,**e**,**g**,**h**) represents an individual mouse (**b**,**c**,**g**), LCs per HPF (**e**) or RLU values (**f**); small horizontal lines indicate

the mean (±s.e.m. in **h**). Scale bars, 50 mu;m (**d**) or 100 mu;m (**f**). *$P < 0.05$ and **$P < 0.0001$ (two-tailed unpaired Student's *t* test (**a**–**c**,**e**) or Tukey's multiple-comparisons test (**g**,**h**)). Data are representative of six independent experiments (**a**; mean + s.e.m) or three independent experiments (**d**,**f**), or are pooled from three independent experiments (**b**,**c**,**e**,**g**) with $n = 5$ mice per group (**d**,**e**) or three to six independent experiments (**h**).

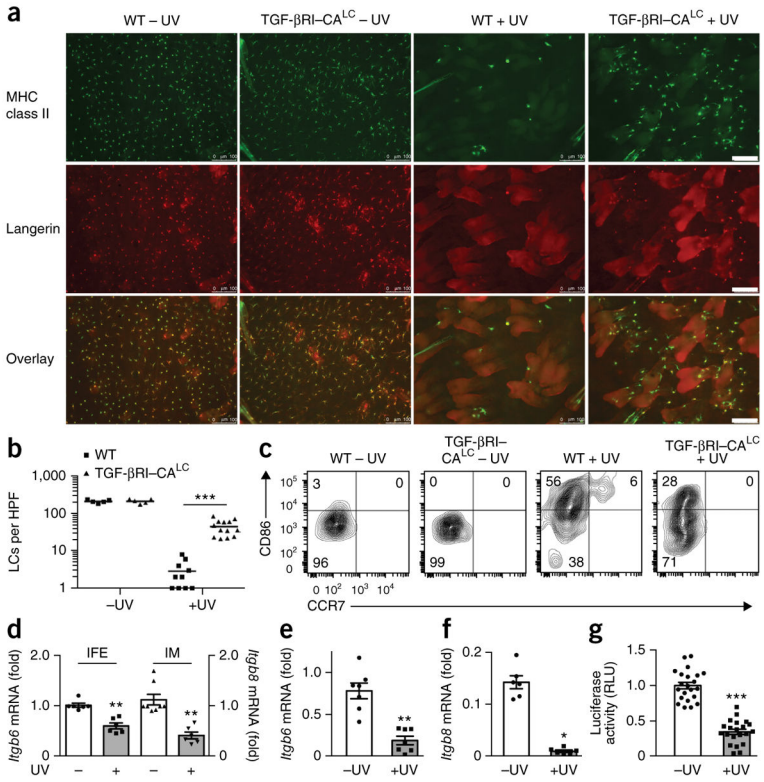

Figure 4.

UV irradiation promotes LC migration through diminished integrin expression and TGF-β activation. (**a**) Microscopy of whole mounts of back epidermis from tamoxifen-treated wild-type and TGF-βRI–CA^{LC} mice (n = 5 per group) 4 d after sham treatment (-UV) or UVB irradiation (+UV), stained for MHC class II (green) and langerin (red). Scale bars, 100 mu;m. (**b**) Quantification of LCs (per HPF) in **a**. (**c**) Flow cytometry analyzing the expression of CD86 and CCR7 by epidermal LCs from mice as in **a**, gated as CD45^{+}MHCII^{+}CD11b^{int} langerin-positive cells. Numbers in quadrants indicate percent cells in each. (**d**) Quantitative RT-PCR analysis of *Itgb6* mRNA (left vertical axis) and *Itgb8* mRNA (right vertical axis) in flow cytometry–sorted populations of IFE and IM KCs from wild-type mice 18 h after sham treatment or UVB irradiation (presented as in Fig. 2e). (**e**,**f**) Quantitative RT-PCR analysis of *Itgb6* mRNA (**e**) and *Itgb8* mRNA (**f**) in mouse primary KC cultures 24 h after sham treatment or UVB irradiation (presented as in Fig. 2e). (**g**) Luciferase activity of mink lung TGF-β reporter cells cultured together with primary keratinocytes given sham treatment or UVB irradiation; results are normalized to those of sham-treated cells. Each symbol (**b**,**d**–**g**) represents LCs per HPF (**b**), an independent experiment (**d**–**f**) or RLU values (**g**); small horizontal lines indicate the mean (±s.e.m. in **d**–**g**). *P < 0.01, **P < 0.001 and ***P < 0.0001 (two-tailed Mann-Whitney test (**b**,**f**) or two-tailed unpaired t test (**d**,**e**,**g**)). Data are representative of three independent experiments (**a**,**c**) or are pooled from three independent experiments with five mice per group (**b**) or six to seven independent experiments (**d**–**g**).

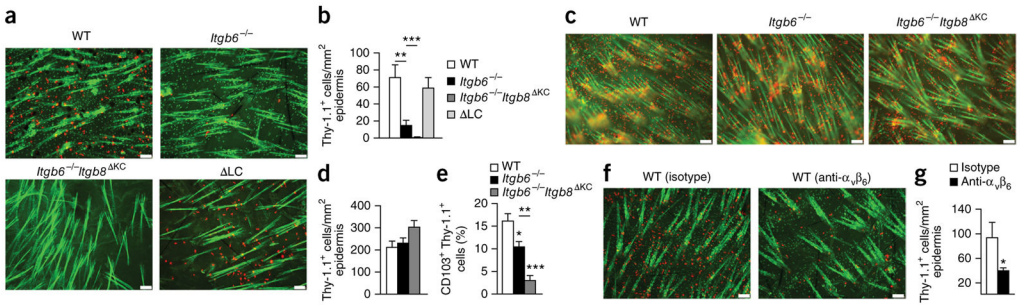

Figure 5.

$\alpha_v\beta_6$ and $\alpha_v\beta_8$ are required for the residence of $CD8^+$ T_{RM} cells in epidermis. (**a**) Microscopy of whole mounts of back epidermis from wild-type, *Itgb6*$^{-/-}$, *Itgb6*$^{-/-}$*Itgb8*$^{\Delta KC}$ and LC-deficient (ΔLC) mice given injection of Thy-1.1^+ P14 cells on day -1 and infected with LCMV on day 0, followed by topical treatment with DNFB on day 3 (for epidermal seeding of P14 T cells), stained for Thy-1.1 (red) and MHC class II (green) on day 42 after infection. (**b**) Quantification of Thy-1.1^+ cells in **a**. (**c**) Microscopy of whole mounts of back epidermis from wild-type, *Itgb6*$^{-/-}$ and *Itgb6*$^{-/-}$*Itgb8*$^{\Delta KC}$ treated as in **a**, stained for Thy-1.1 (red) and MHC class II (green) on day 7 after infection. (**d**) Quantification of Thy-1.1^+ cells in **c**. (**e**) Frequency of $CD103^+$Thy-1.1^+ cells in epidermis of the mice in **c**, assessed by flow cytometry on day 7 after infection. (**f**) Microscopy of whole mounts of back epidermis from wild-type mice treated intraperitoneally with anti-$\alpha_v\beta_6$ or isotype-matched control antibody once a week for 4 weeks starting at 56 d after infection with LCMV and epidermal seeding of T_{RM} cells as in **a**, stained for Thy-1.1 (red) and MHC class II (green). (**g**) Quantification of Thy-1.1^+ cells in **f**. Autofluorescent hair follicles are visible in **a**,**c**,**f**. Scale bars (**a**,**c**,**f**), 100 μm. $*P < 0.05$, $**P < 0.01$ and $***P < 0.0001$ (Tukey's multiple-comparisons test (**b**,**e**) or two-tailed Mann-Whitney test (**g**)). Data are representative of two to three independent experiments with $n = 4$ mice per group (**a**,**b**; mean + s.e.m. in **b**) or two independent experiments with $n = 4$–5 mice per group (**c**–**g**; mean + s.e.m. in **d**,**e**,**g**).

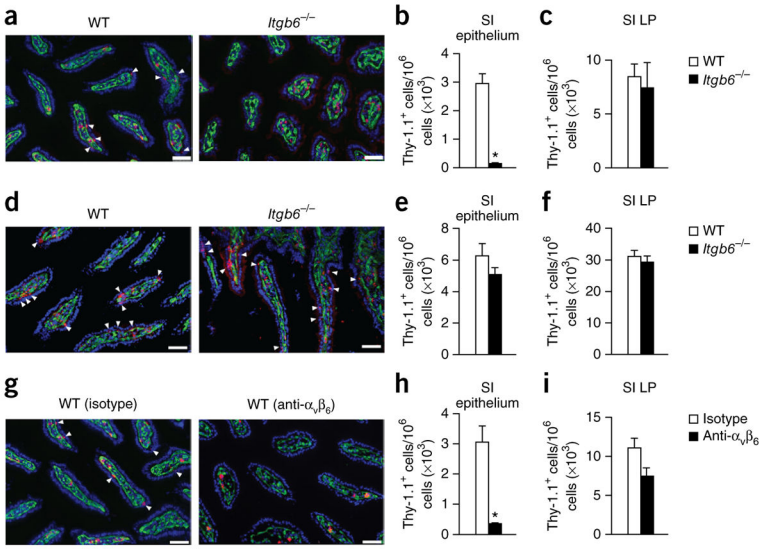

Figure 6.

$\alpha_v\beta_6$ is required for residence of T_{RM} cells in intestinal epithelium. (**a**) Microscopy of small intestine from wild-type and *Itgb6*$^{-/-}$ mice 42 d after infection with LCMV, stained for Thy-1.1 (red) and collagen IV (ColIV) (green) and with DAPI (blue); arrowheads indicate T_{RM} cells in the epithelial layer. (**b**,**c**) Quantification of Thy-1.1$^+$ cells (per 10^6 nucleated cells) in the epithelial layer (above collagen IV (arrowheads) in **a**) (**b**) and lamina propria (LP) (below collagen IV in **a**) (**c**) of the small intestine (SI) of mice as in **a**. (**d**) Microscopy of small intestine from wild-type and *Itgb6*$^{-/-}$ mice 7 d after infection with LCMV, stained as in **a**. (**e**,**f**) Quantification of Thy-1.1$^+$ cells in the epithelial layer (as in **b**) (**e**) and lamina propria (as in **c**) (**f**) of the small intestine of mice as in **d**. (**g**) Microscopy of small intestine from wild-type mice infected with LCMV and then treated intraperitoneally with anti-$\alpha_v\beta_6$ or isotype-matched control antibody starting at 56 d after infection, stained as in **a**. (**h**,**i**) Quantification of Thy-1.1$^+$ cells in the epithelial layer (as in **b**) (**h**) and lamina propria (as in **c**) (**i**) of the small intestine of mice as in **g.** Scale bars (**a**,**d**,**g**), 50 μm. *$P < 0.05$ (two-tailed Mann-Whitney test). Data representative of three independent experiments with $n = 4$ mice per group (**a**–**c**; mean + s.e.m. in **b**,**c**) or two independent experiments with $n = 4$–5 mice per group (**d**–**i**; mean + s.e.m. in **e**,**f**,**h**,**i**).